1521-009X/49/5/369–378$35.00
Drug Metabolism and Disposition

https://doi.org/10.1124/dmd.121.000385
Drug Metab Dispos 49:369–378, May 2021

Tertiary Oxidation of Deoxycholate Is Predictive of CYP3A Activity in Dogs

Wushuang Zeng,[1] Lanlan Gui,[1] Xianwen Tan, Pingping Zhu, Yiting Hu, Qingliang Wu, Xuejing Li, Lian Yang, Wei Jia, Changxiao Liu, and Ke Lan

Key Laboratory of Drug Targeting and Drug Delivery System, Ministry of Education, West China School of Pharmacy, Sichuan University, Chengdu, China (W.Z., L.G., X.T., P.Z., Y.H., Q.W., K.L.); Chengdu Health-Balance Medical Technology Co., Ltd., Chengdu, China (X.L., L.Y., K.L.); WestChina-Frontier PharmaTech Co., Ltd., Chengdu, China (L.Y.); School of Chinese Medicine, Hong Kong Baptist University, Kowloon Tong, Hong Kong, China (W.J.); and State Key Laboratory of Drug Delivery Technology and Pharmacokinetics, Tianjin Institute of Pharmaceutical Research, Tianjin, China (C.L.)

Received January 20, 2021; accepted February 26, 2021

ABSTRACT

Deoxycholic acid (DCA, 3α, 12α-dihydroxy-5β-cholan-24-oic acid) is the major circulating secondary bile acid, which is synthesized by gut flora in the lower gut and selectively oxidized by CYP3A into tertiary metabolites, including 1β,3α,12α-trihydroxy-5β-cholan-24-oic acid (DCA-1β-ol) and 3α,5β,12α-trihydroxy-5β-cholan-24-oic acid (DCA-5β-ol) in humans. Since DCA has the similar exogenous nature and disposition mechanisms as xenobiotics, this work aimed to investigate whether the tertiary oxidations of DCA are predictive of in vivo CYP3A activities in beagle dogs. In vitro metabolism of midazolam (MDZ) and DCA in recombinant canine CYP1A1, 1A2, 2B11, 2C21, 2C41, 2D15, 3A12, and 3A26 enzymes clarified that CYP3A12 was primarily responsible for either the oxidation elimination of MDZ or the regioselective oxidation metabolism of DCA into DCA-1β-ol and DCA-5β-ol in dog liver microsomes. Six male dogs completed the CYP3A intervention studies including phases of baseline, inhibition (ketoconazole treatments), recovery, and induction (rifampicin treatments). The oral MDZ clearance after a single dose was determined on the last day of the baseline, inhibition, and induction phases, and subjected to correlation analysis with the tertiary oxidation ratios of DCA detected in serum and urine samples. The results confirmed that the predosing serum ratios of DCA oxidation, DCA-5β-ol/DCA, and DCA-1β-ol/DCA were significantly and positively correlated both intraindividually and interindividually with oral MDZ clearance. It was therefore concluded that the tertiary oxidation of DCA is predictive of CYP3A activity in beagle dogs. Clinical transitional studies following the preclinical evidence are promising to provide novel biomarkers of the enterohepatic CYP3A activities.

SIGNIFICANCE STATEMENT

Drug development, clinical pharmacology, and therapeutics are under insistent demands of endogenous CYP3A biomarkers that avoid unnecessary drug exposure and invasive sampling. This work has provided the first proof-of-concept preclinical evidence that the CYP3A catalyzed tertiary oxidation of deoxycholate, the major circulating secondary bile acid synthesized in the lower gut by bacteria, may be developed as novel in vivo biomarkers of the enterohepatic CYP3A activities.

Introduction

CYP3A is the most important class of drug-metabolizing enzymes, which has the highest catalytic promiscuity index among P450 enzymes (Foti et al., 2011). It's well known that 46% of clinically used drugs are metabolized via CYP3A (Wienkers and Heath, 2005). Rendic and Guengerich (2015) recently updated the data by covering a much broader range of chemicals, proposing that CYP3A4 and CYP3A5 participate in metabolic reactions of 20% and 4% for general chemicals and 27% and 6% for drugs marketed and under development, respectively. More importantly, there is not only a great interindividual but also a high intraindividual variability of the variants, transcription, and translation of CYP3A genes in adult liver and intestine due to their susceptibility of inhibition and induction (Zanger and Schwab, 2013). Such variations bring great challenges to maintain an expected exposure of drugs primarily metabolized by CYP3A, resulting in great variability of drug response and serious drug-drug interaction–associated adverse

This work was supported by the National Natural Science Foundation of China [Grant 82073921] and partly by the Fundamental Research Funds for the Central Universities and the 111 Project of the National Ministry of Education [Grant B18035].

The authors declare no conflict of interest.

[1]W.Z. and L.G. contributed equally to this work.

https://doi.org/10.1124/dmd.121.000385.

ABBREVIATIONS: ALP, alkaline phosphatase; ALT, alanine transaminase; AST, aspartate aminotransferase; $AUC_{0-\infty}$, area under curve from zero to infinity; BA, bile acid; CA, cholic acid; CDCA, chenodeoxycholic acid; *CL/F*, bioavailability corrected clearance; CLZ, clozapine; DCA, deoxycholic acid; DCA-1β-ol, 1β,3α,12α-trihydroxy-5β-cholan-24-oic acid; DCA-5β-ol, 3α,5β,12α-trihydroxy-5β-cholan-24-oic acid; dLM, dog liver microsomes; 4-OH-MDZ, 4-hydroxy-midazolam; GDCA, glycodeoxycholate; HDCA, hyodeoxycholic acid; HLM, human liver microsomes; KTZ, ketoconazole; LCA, lithocholic acid; LC-MS/MS, liquid chromatography with tandem mass spectrometry; MDZ, midazolam; NADPH-A, NADPH-regenerating system solution A; NADPH-B, NADPH-regenerating system solution B; 6β-OHF, 6β-hydroxycortisol; 6β-OHF/cortisol, 6β-hydroxycortisol-to-cortisol; 1′-OH-MDZ, 1′-hydroxymidazolam; P450, cytochrome P450; RFP, rifampicin; $T_{1/2}$, terminal half-life; TBA, total bile acid; TDCA, taurodeoxycholate; QC, quality control.

events. Drug development, clinical pharmacology, and therapeutics are under insistent demands of validated biomarkers for the detection of in vivo CYP3A activities.

Several exogenous probe substrates have been developed to assess the in vivo activities of CYP3A. Midazolam (MDZ) is a selective substrate of CYP3A4 and CYP3A5 (Gorski et al., 1994; Patki et al., 2003) whose oral clearance is widely accepted as the gold standard to assess the in vivo activities of CYP3A4 and CYP3A5. The erythromycin breath test involves intravenous administration of ^{14}C-erythromycin, whose *N*-demethylation is a marker reaction of CYP3A4 (Gonzalez, 1990) and the measurement of $^{14}CO_2$ in the breath (Rivory et al., 2001; Rivory and Watkins, 2001). This erythromycin breath test is less invasive, however, omits the intestinal CYP3A activities, and sometimes showed discrepant results with the MDZ method (Kinirons et al., 1999). Another ideal strategy is to develop endogenous CYP3A biomarkers, which is greatly advantaged by avoiding unnecessary drug exposure and invasive sampling. The urinary 6β-hydroxycortisol-to-cortisol (6β-OHF/cortisol) ratio was the first endogenous marker (Ged et al., 1989) and has shown correlation with intravenous MDZ clearance (Shin et al., 2016). This biomarker has huge individual variations because it is involved in glucocorticoid metabolism and is susceptive to influence from other nonCYP3A factors such as stress, infections, and circadian rhythm (Galteau and Shamsa, 2003). Plasma 4β-hydroxycholesterol was another surrogate of CYP3A activities (Bodin et al., 2001) and also showed correlations with MDZ clearance in humans (Kasichayanula et al., 2014; Gravel et al., 2019). However, the long half-life of 4β-hydroxycholesterol resulted in limitations to assess the short-term CYP3A inhibition status (Diczfalusy et al., 2011; Kasichayanula et al., 2014). Because of the limited predictive capability of single biomarkers, recent works tried to develop combinatory biomarkers based on bioinformatic tools (Shin et al., 2013; Kim et al., 2018).

Deoxycholic acid (DCA, 3α, 12α-dihydroxy-5β-cholan-24-oic acid) is a secondary bile acid (BA) that is synthesized by gut bacteria via 7-dehydroxylation of cholic acid (CA, 3α, 7α, 12α-trihydroxy-5β-cholan-24-oic acid), the primary BA synthesized in liver (Russell, 2003). We've recently disclosed that human CYP3A4 and CYP3A7 are exclusively responsible for the tertiary oxidations of DCA, glycodeoxycholate (GDCA), and taurodeoxycholate (TDCA) regioselectively at C-1β, C-6α, C-5β, C-4β, C-6β, and C-19 (Zhang et al., 2019). Correlation between DCA oxidations and testosterone 6β-hydroxylation in single-donor adult liver microsomes found that DCA oxidations at C-1β, C-5β, and C-6α were good indicators for in vitro CYP3A4 activities (Chen et al., 2019). Subsequent studies of interspecies difference confirmed that the tertiary oxidation of DCA is conserved in common preclinical animals including mice, rats, beagle dogs, and monkeys (Lin et al., 2020). However, the BA metabolism of murine animals is quite different from that of human, not only in the downstream oxidative metabolism of CDCA (chenodeoxycholic acid) but also in the regioselectivity of DCA oxidations. In contrast, beagle dogs have a similar BA metabolism network as humans, particularly in the oxidation of DCA at C-1β and C-5β (Lin et al., 2020). Beagle dogs may therefore be suitable to investigate whether DCA oxidation may serve as novel biomarkers of CYP3A activities.

The canine CYP3A family comprises two isoforms, CYP3A12 and CYP3A26 (Fraser et al., 1997; Mealey et al., 2019). Beagle dogs have been widely used as preclinical animals for CYP3A associated drug-drug interaction studies (Abramson and Lutz, 1986; Kyokawa et al., 2001; Graham et al., 2002; Kuroha et al., 2002; Mills et al., 2010) and it is generally accepted that MDZ is a probe substrate of CYP3A for both dogs and humans (Martinez et al., 2013). However, Locuson et al. (2019) suggested that MDZ might not be a sensitive probe for canine CYP3A because MDZ was oxidized into 1′-hydroxymidazolam (1′-OH-MDZ) more by canine CYP2B11 than 3A12 (Locuson et al. 2009). In this work, we compared in vitro metabolism of MDZ, cortisol, and DCA in the recombinant canine P450 enzymes and confirmed that CYP3A12 rather than 2B11 is the major isoform responsible for the oxidative degradation of MDZ and DCA. We performed correlation studies of the predosing DCA oxidation biomarkers in serum with either the urinary 6β-OHF/cortisol or the oral MDZ clearance after oral ketoconazole (KTZ, a strong CYP3A inhibitor) and oral rifampicin (RFP, a strong CYP3A inducer) treatments in beagle dogs. Data obtained in this work provided proof-of-concept evidence that the tertiary oxidation of DCA is predictive of CYP3A activity in beagle dogs.

Materials and Methods

Materials and Reagents. Authentic standards of CA, DCA, CDCA, LCA (3α-hydroxy-5β-cholan-24-oic acid), HDCA (3α, 6α-dihydroxy-5β-cholan-24-oic acid), and stable isotope-labeled internal standards (CA-2,2,4,4-D4, DCA-2,2,4,4-D4, UDCA-2,2,4,4-D4, and LCA-2,2,4,4-D4) were obtained from Steraloids (Newport, RI), TRC (Toronto), or Sigma-Aldrich (St. Louis, MO) as previously described (Zhu et al., 2018). DCA-1β-ol and DCA-5β-ol were synthesized as described in our recent report (Zhang et al., 2019). MDZ was purchased from Cerilliant (Austin, TX, United States) and 1′-OH-MDZ was purchased from MedChem Express (New Jersey). Authentic standards of cortisol, 6β-OHF, cortisol-D4, and clozapine (CLZ) were obtained from Sigma-Aldrich. Progesterone was purchased from Nine-Dinn Chemistry (Shanghai, China). Choloylglycine hydrolase from clostridium perfringens, sulfatase, and β-glucuronidase from Helix pomatia Type H-1 were purchased from Sigma-Aldrich. Liquid chromatograph-mass spectrometry grade methanol, acetonitrile, formic acid, and sodium acetate were purchased from Sigma-Aldrich. DMSO was purchased from Thermo Fisher Scientific (Waltham, MA). Ultra-pure water was obtained by using a Milli-Q system (Bedford, MA).

The pooled human liver microsomes (HLMs) (catalog 452117, lot 38291) from 150 mixed-gender adult donors, the pooled dog liver microsomes (dLMs) (catalog 452602, lot 7026001 from three female dogs; catalog 452601, lot 6116002 from four male dogs) from seven mixed-gender donors, NADPH-regenerating system solution A (NADPH-A, containing 26 mM $NADP^+$, 66 mM glucose-6-phosphate and 66 mM $MgCl_2$ in water), NADPH-regenerating system solution B (NADPH-B, containing 40 U/ml glucose-6-phosphate dehydrogenase in 5 mM sodium citrate), and 0.5 M pH 7.4 PBS were purchased from Corning (Tewksbury, MA). The recombinant canine CYP1A1, 1A2, 2B11, 2C21, 2C41, 2D15, 3A12, and 3A26 enzymes prepared from plasmid-transfected Escherichia coli (Bactosomes) were obtained from Cypex Ltd. (Dundee, Scotland, UK).

MDZ tablets (15 mg, lot 20170402; Jiangsu Nhwa Pharmaceutical Co., Ltd.) and RFP capsules (300 mg, lot 171104; Chengdu Jinhua Pharmaceutical Co., Ltd.) were gifted by the Pharmacy Department of the Fourth People's Hospital of Chengdu. KTZ from Aladdin Bio-Chem Technology Co., Ltd. (Shanghai, China) and sodium carboxymethyl cellulose from Sigma-Aldrich were used for dog intervention studies.

In Vitro Metabolism Assay of MDZ, Cortisol, and DCA. In vitro metabolism of MDZ, cortisol, and DCA were assessed using the published protocols (Chen et al., 2019; Zhang et al., 2019). In brief, incubations were performed in 96-well plates in a shaking incubator at 37°C. The 100-μl incubation system contained 0.1 M PBS (pH 7.4), 5.0 μl NADPH-A, 1.0 μl NADPH-B, 1.0 μl substrate working solution, and an appropriate volume of dog liver microsomes or recombinant canine P450 enzymes. For MDZ incubations, the initial substrate levels were 4 and 40 μM, and the microsome protein concentration was 0.1 mg protein/ml. For cortisol incubations, the substrate level was 10 μM, and the microsome protein concentration was 0.5 mg protein/ml. For DCA incubations, the substrate level was 50 μM, and the microsome protein concentration was 0.5 mg protein/ml. The recombinant P450 protein concentration was 50 pmole/ml. All incubations were performed in triplicates. The reactions were initiated by adding liver microsomes or recombinant enzymes and subsequently stopped at 10, 120, and 120 minutes for incubations of MDZ, cortisol, and DCA, respectively, by adding 300 μl ice-cold acetonitrile containing internal standards, 82.5 nM CLZ, 330 nM progesterone, and 50 nM CA-2,2,4,4-D4, respectively. The samples were centrifuged at 4°C at 4000*g* for 20 minutes. The supernatant was diluted with 50% acetonitrile and subjected to LC-MS/MS analysis.

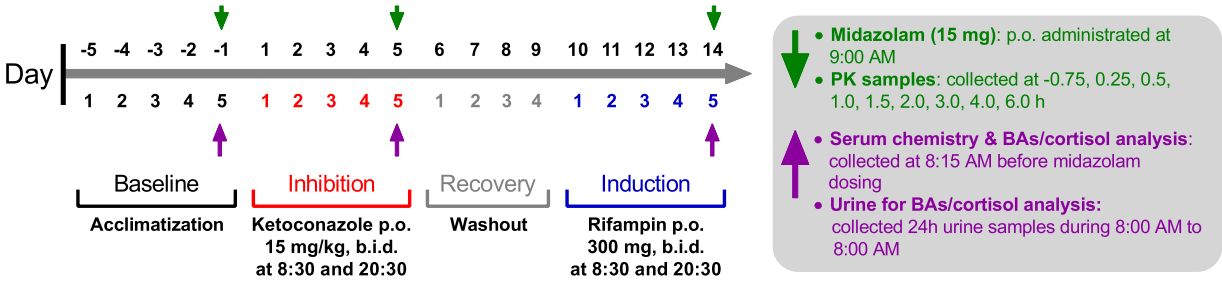

Fig. 1. Scheme of the CYP3A intervention studies including the baseline phase, inhibition phase, recovery phase, and induction phase in six male beagle dogs. p.o., peroral.

In Vitro Inhibition of KTZ on DCA Oxidations in Dog Liver Microsomes. Inhibition of KTZ on DCA oxidations in dog liver microsomes was performed as previous protocols (Chen et al., 2019; Zhang et al., 2019). The 100-μl incubation system contained 0.1 M PBS (pH 7.4), 5.0 μl NADPH-A, 1.0 μl NADPH-B, 0.5 μl DCA working solution in DMSO, 0.5 μl KTZ solution in DMSO, and 2.5 μl liver microsomes (protein concentration of 20 mg/ml). The final concentration was 0.5 mg protein/ml for liver microsomes, 50 μM for DCA, and 0.001, 0.01, 0.03, 0.1, 0.5, 1, 5, and 30 μM for KTZ in the incubation media. All incubations were performed in triplicates. The reactions were stopped at 60 minutes by adding 300 μl ice-cold acetonitrile containing CA-2,2,4,4-D4 (50 nM) and centrifuged at 4°C at 4000*g* for 20 minutes. The supernatant was diluted with water and subjected to LC-MS/MS analysis.

In Vivo Intervention Studies of CYP3A in Dogs. All the animal experiments were approved by the Animal Experimental Ethics Committee of West China Medical Center, Sichuan University. Six 1-year-old male beagle dogs with body weight of 7–10 kg were obtained from WestChina-Frontier PharmaTech Co., Ltd. (Chengdu, China). They were raised with controlled temperature, humidity, ventilation, and illumination, allowed access to water ad libitum, and given food once daily at noon. As shown in Fig. 1, the intervention studies included four sequential phases of baseline, inhibition, recovery, and induction. After a 5-day acclimatization phase (day −5 ~ day −1), dogs were given multiple oral doses (day 1 ~ day 5) of KTZ (15 mg/kg, b.i.d., at 8:30 and 20:30), which was suspended in 0.5% carboxymethyl cellulose at a concentration of 15 mg/ml. After a 4-day wash out phase (day 6 ~ day 9) after the inhibition phase, dogs were given multiple oral doses (day 10 ~ day 14) of RFP (300 mg, b.i.d., at 8:30 and 20:30). A single oral dose of MDZ (15 mg) was given to dogs on day −1 (baseline phase), day 5 (inhibition phase), and day 14 (induction phase) at 9:00 to evaluate the in vivo activity of CYP3A. On each day of MDZ dosing, blood samples (1 ml) were collected before MDZ administration, and the 24-hour urine samples were collected after MDZ administration for analysis of cortisol, 6β-OHF, and BAs. After each MDZ dosing, blood samples (1 ml) were collected for MDZ pharmacokinetic analysis in heparinized tubes at −0.75, 0.25, 0.5, 1.0, 1.5, 2.0, 3.0, 4.0, and 6.0 hours. The blood samples were centrifuged at 4°C at 2000*g* for 10 minutes to separate serum and plasma samples. All samples were stored at −80°C until analysis.

Serum Chemistry Tests. Serum chemistry tests of alanine transaminase (ALT), aspartate aminotransferase (AST), alkaline phosphatase (ALP), and total bile acid (TBA) were carried out at the laboratory of WestChina-Frontier PharmaTech Co., Ltd. on the Roche Cobas C311 automatic chemical analyzer. ALT, AST, and ALP were measured by the International Federation and Clinical Chemistry reference method, and TBA was measured by the enzymatic cycling method.

Quantitative Determination of MDZ in Plasma. Plasma MDZ levels were determined on an ACQUITY ultra-performance liquid chromatography machine coupled to a Xevo TQ-S mass spectrometer (Waters, Milford, MA) equipped with an ACQUITY BEH C18 column (1.7 μm, 50 × 2.1 mm) (Waters) maintained at 35°C. In brief, 325 μl acetonitrile containing 0.1% formic acid and 30 ng/ml CLZ were added into 25 μl plasma samples. The samples were vortex mixed at 1500 rpm for 4 minutes and centrifuged at 4°C at 3000*g* for 30 minutes. The supernatant (100 μl) was diluted with 300 μl of 50% methanol-water and subjected to analysis. The mobile phases consisted of 0.1% formic acid in water (mobile phase A) and acetonitrile (mobile phase B). The injection volume was 1 μl, and the flow rate was 0.50 ml/min with gradient as follows: 0.0–0.7 minutes (20%–80% B), 0.7–1.1 minutes (80–98% B), and 1.1–1.6 minutes (80% B). With capillary voltage of 3.0 kV, source temperature of 150°C, desolvation temperature of 550°C, cone gas flow of 150 L/h, desolvation gas flow of 950 l/h, and collision energy of 25 V, MDZ and CLZ were detected in positive mode at selected ion transients of 326 > 291 and 327 > 192, respectively. The calibration samples (5–5000 ng/ml) and quality control (QC) samples (20, 1000, 3000 ng/ml) prepared in pooled blank dog plasma were allocated into each bioanalytical run, in which the bias of all QC samples was within ± 15%.

Detection of MDZ Metabolites in Incubation Media. MDZ and its hydroxylated metabolites including 1′-OH-MDZ and 4-hydroxy-midazolam (4-OH-MDZ) in the incubation media were detected on the same instrument with slight modifications. The same mobile phases were used with the gradient adjusted to improve separation of MDZ, 1′-OH-MDZ, and 4-OH-MDZ as follows: 0.0–1.1 minutes (30%–95% B), 1.1–1.4 minutes (95% B), and 1.4–1.6 minutes (30% B). MDZ, 1′-OH-MDZ/4-OH-MDZ, and CLZ were detected in positive mode at selected ion transients of 326 > 291, 342 > 297, and 327 > 192, respectively. The response ratios of their peak areas to that of CLZ were used to evaluate the degradations of MDZ and the formations of 1′-OH-MDZ or 4-OH-MDZ in dLM and recombinant canine P450 enzymes.

Quantitative Determination of Cortisol and 6β-OHF. Cortisol and 6β-OHF in serum and urine samples were determined on the same LC-MS/MS instruments equipped with an ACQUITY HSS T3 column (1.8 μm, 50 × 2.1 mm) (Waters) maintained at 40°C. In brief, 500 μl ethyl acetate containing 2 ng/ml cortisol-D4 were added into 50 μl serum or urine samples. The samples were vortex mixed at 1500 rpm for 10 minutes and centrifuged at 4°C at 18,000*g* for 30 minutes. The supernatant (400 μl) was vacuum-evaporated at 40°C, reconstituted with 100 μl water-methanol (50:50, v/v), and subjected to analysis. The mobile phases consisted of 0.01% formic acid in water (mobile phase A) and 0.01% formic acid in methanol (mobile phase B). The injection volume was 5 μl and the flow rate was 0.40 ml/min with gradient as follows: 0.0–0.3 minutes (80% A), 0.3–4.0 minutes (80%–5% A), 4.0–4.7 minutes (5% A), and 4.7–5.0 minutes (5%–80% A). At capillary voltage of 3.5 kV, cortisol and 6β-OHF were detected in positive mode at selected ion transients of 363 > 121 and 379 > 325, with a collision energy of 24 eV and 14 eV, respectively. The calibration samples (0.5–200.0 ng/ml for cortisol and 5–2000 ng/ml for 6β-OHF) and QC samples (1.5, 20.0, 100.0, and 150.0 ng/ml for cortisol and 15, 200 1000, and 1500 ng/ml for 6β-OHF) prepared in 0.1 M PBS (pH 7.4) were allocated into each bioanalytical run, in which the bias of all QC samples was within ± 15%. Cortisol and 6β-OHF were detected in the incubation media with the same method except that progesterone was used as internal standard (m/z 315 > 109).

Quantitative Determination of BAs. Quantitative analysis of unconjugated BAs was performed as previously described (Yin et al., 2017; Zhu et al., 2018). In a 96-well plate, 150 μl sodium acetate buffer (pH 5.0) containing 100 U choloylglycine hydrolase, 50 U sulfatase, and 500 U β-glucuronidase was added into 50 μl serum or urine. The plate was incubated at 37°C for 6 hours and subsequently lyophilized to deconjugate the *N*-acylamidated, sulfated, and/or glucuronidated forms of BAs. 200 μl acetonitrile containing 1% formic acid and 100 nM internal standards was added into each well. The plate was then vortex mixed at 1500 rpm at 10°C for 30 minutes and centrifuged at 4°C at 3000*g* for 20 minutes. The supernatant (200 μl) was vacuum-evaporated at 30°C, reconstituted with 100 μl water-acetonitrile (50:50, v/v), and subjected to analysis. The mobile phases consisted of 0.01% formic acid in water (mobile phase A) and acetonitrile (mobile phase B). The injection volume was 5 μl, and the flow rate was 0.45 ml/min with the following mobile phase gradient: 0.0–0.5 minutes (95% A), 0.5–1.0 minutes (95%–64% A), 1.0–2.0 minutes (64%–74% A), 2.0–4.0 minutes (74%–70% A), 4.0–6.0 minutes (70% A), 6.0–7.0 minutes (70%–62% A), 7.0–9.0 minutes (62%–55% A), 9.0—12.5 minutes

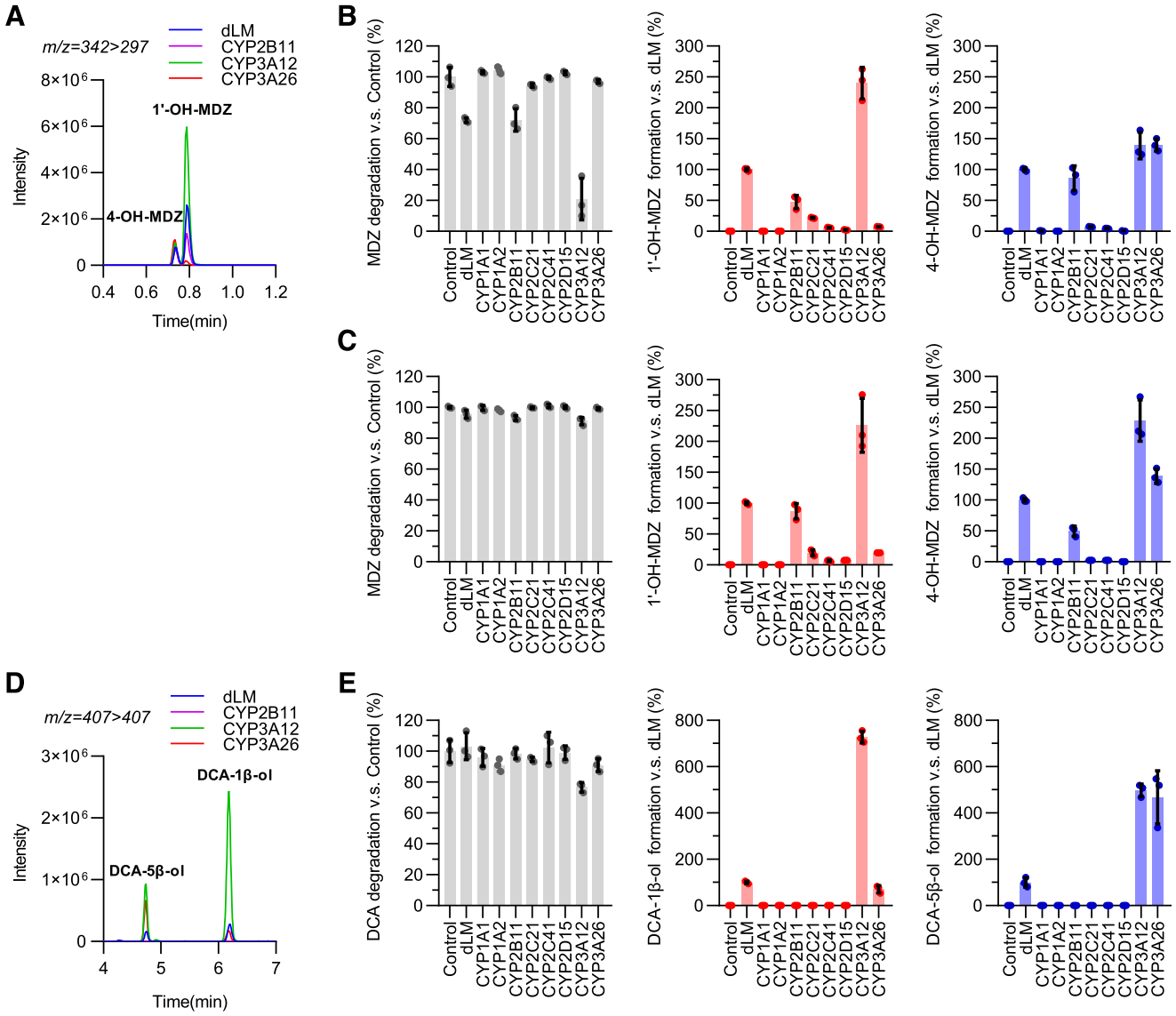

Fig. 2. CYP3A12 is primarily responsible for both the oxidation elimination of MDZ and the regioselective oxidation metabolism of DCA in dLMs. The representative ion chromatograms of oxidative metabolites of MDZ (A) and DCA (D) were detected after incubation for 10 and 120 minutes, respectively, in dog liver microsomes (0.1 mg protein/ml for MDZ; 0.5 mg protein/ml for DCA) and recombinant canine P450 enzymes (50 pmol protein/ml). The percentage degradation rates and metabolite formation rates of MDZ at 4 μM (B), 40 μM (C), and DCA at 50 μM (D) in a panel of eight canine P450 enzymes were calculated in comparison with the control data (without addition of dLM) and the dLM data, respectively. Data were shown as mean ± S.D. (n = 3).

(55%–30% A), 12.5–13.0 minutes (30%–0% A), 13.0–14.0 minutes (0% A), 14.0–14.1 minutes (0%–95% A), and 14.1–15.0 minutes (95% A). Selected ion recorded in negative mode for the quantification and identification of unconjugated BAs was described in our previous reports (Lan et al., 2016; Yin et al., 2017; Zhu et al., 2018; Zhang et al., 2019).

Data Processing. The LC-MS/MS raw data were processed by UNIFI (V1.8, Waters, Milford, MA, United States) and MassLynx (V4.1, Waters, Milford, MA, United States). Pharmacokinetic parameters of MDZ were calculated by Phoenix WinNonlin (V7.0, Pharsight) according to noncompartment model, including C_{max}, area under curve from zero to infinity ($AUC_{0-\infty}$), terminal half-life, ($T_{1/2}$) and bioavailability-corrected clearance (CL/F). Calculation of IC_{50} value of KTZ on DCA oxidations, paired-sample t tests of serum chemistry data, MDZ pharmacokinetic parameters, serum/urine levels, and metabolic ratios of BAs and cortisol, as well as their correlation analysis, were conducted by GraphPad Prism software (V7.0; GraphPad Software, LaJolla, CA). The interindividual Pearson correlation analysis of either DCA oxidation ratios or 6β-OHF/cortisol ratio with MDZ clearance was performed for all data of six dogs, and the intraindividual Pearson correlation analysis was performed for data acquired from each dog.

Results

Oxidations of MDZ, Cortisol, and DCA in Recombinant Canine P450 Enzymes. Eight canine P450 enzymes were investigated in comparison with dLM to identify the major isoform responsible for the oxidation metabolism of MDZ, cortisol, and DCA. Fig. 2, A–C showed the oxidation metabolism of MDZ (4 and 40 μM) in recombinant canine P450 enzymes (50 pmole/ml) and dLM (0.1 mg/ml). The oxidative degradation of MDZ in dLM, which involved 1′-hydroxylation and 4-hydroxylation (Fig. 2A), was ascribed primarily to CYP3A12, secondly to CYP2B11 and CYP3A26, and minorly to CYP2C21 at substrate concentrations of 4 μM (Fig. 2B) and 40 μM (Fig. 2C). Toward MDZ 1′-hydroxylation, CYP3A12 exhibited about 5.0- and 11.0-fold higher activities than CYP2B11 and 2C21 at 4 μM, and 2.6- and 11.6-fold higher activities than CYP2B11 and 2C21 at 40 μM, respectively. CYP2B11, 3A12, and 3A26 were also involved in MDZ 4-hydroxylation, in which CYP3A12 and 3A26 showed comparable

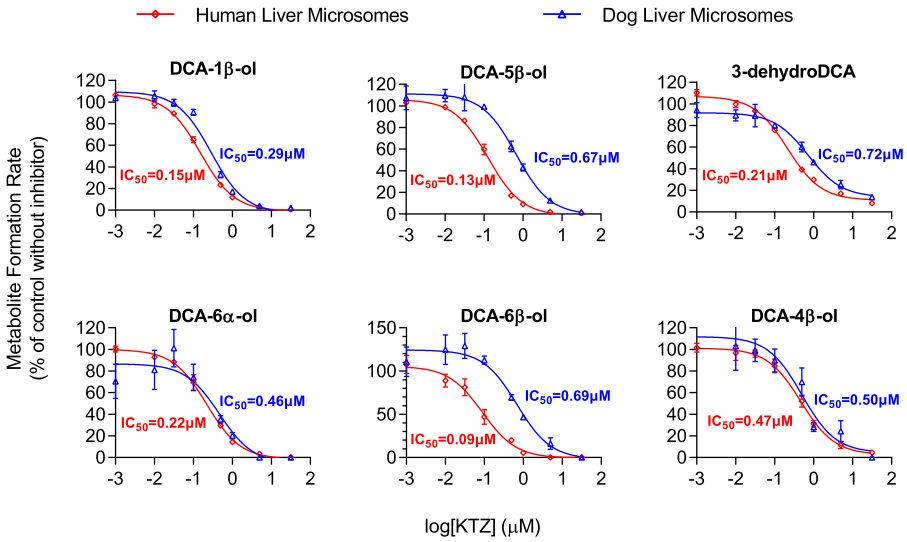

Fig. 3. Inhibition of ketoconazole on the oxidations of DCA (50 μM) in the pooled liver microsomes of dogs and humans. Data were shown as mean ± S.D. (n = 3).

and higher activities than CYP2B11 at substrate concentration at both 4 and 40 μM. Fig. 2, D and E showed the oxidation metabolism of DCA (50 μM) in canine P450 enzymes (50 pmole/ml) and dLM (0.5 mg/ml). The oxidative degradation of DCA in dLM, which mainly involved 1β-hydroxylation and 5β-hydroxylation (Fig. 2C), was ascribed exclusively to CYP3A12 and 3A26 (Fig. 2D). In comparison with CYP3A26, CYP3A12 showed much higher activities toward DCA 1β-hydroxylation and comparable activities toward 5β-hydroxylation. As for the oxidation metabolism of cortisol, we did not detect the formation of 6β-OHF in either dLM or any canine P450 enzymes (data not shown).

Inhibitory Effects of KTZ on DCA Oxidations in Liver Microsomes. The inhibitory effects of KTZ on DCA oxidations in dLM were compared with the previous data obtained in HLM (Chen et al., 2019). As shown in Fig. 3, the IC_{50} values of KTZ were 0.15 and 0.29 μM for DCA 1β-hydroxylation, 0.13 and 0.67 μM for DCA 5β-hydroxylation, 0.21 and 0.72 μM for DCA 3β-oxidation, 0.22 and 0.46 μM for DCA 6α-hydroxylation, 0.09 and 0.69 μM for DCA 6β-hydroxylation, and 0.47 and 0.50 μM for DCA 4β-hydroxylation in HLM and dLM, respectively. The data indicated that KTZ possessed similar inhibitory effects on the regioselective oxidations of DCA in dog and human.

Alteration of Liver Functions by KTZ and RFP in Dogs. All six beagle dogs completed the CYP3A intervention studies. The body weights of dogs along the intervention phases showed no statistical difference (data not shown). The serum ALT, AST, ALP, and TBA measured prior to MDZ dosing at the baseline phase, inhibition phase, and induction phase were shown in Fig. 4A. Compared with the baseline data, the KTZ treatments did not change the serum levels of ALT, AST, ALP, or TBA. The RFP treatments also did not change the serum levels of ALT or AST but led to a significant increase of serum ALP and TBA compared with baseline data.

Inhibition and Induction of Oral MDZ Clearance by KTZ and RFP. The pharmacokinetic parameters of MDZ after a single oral dose (15 mg) acquired at the baseline phase, inhibition phase, and induction phase were shown in Fig. 4A. The C_{max} of MDZ increased from 101 ± 39 ng/ml at the baseline to 689 ± 326 ng/ml after the KTZ treatments and reduced to 29 ± 11 ng/ml after the RFP treatments. The $AUC_{0-\infty}$ of MDZ increased from 106 ± 24 to 1332 ± 383 ng*h/ml after the KTZ treatments and reduced to 46 ± 19 ng*h/ml after the RFP treatments. The $T_{1/2}$ of MDZ increased from 0.8 ± 0.1 to 1.6 ± 0.5 hours after the KTZ treatments and recovered to 1.1 ± 0.3 hours after the RFP treatments. As a result, the KTZ treatments significantly reduced the MDZ clearance from 288 ± 89 to 23 ± 8 ml/min/kg, whereas the RFP treatments significantly enhanced the MDZ clearance to 677 ± 237 ml/min/kg. The MDZ clearance data indicated that the CYP3A activities were successfully inhibited and induced at the corresponding intervention phases.

Alteration of BA and Cortisol Levels by KTZ and RFP in Dogs. The serum levels of representative BAs determined prior to MDZ administration at the baseline phase, inhibition phase, and induction phase were shown in Fig. 4C. According to the primary-secondary-tertiary metabolism axis, the BAs included CDCA, LCA, and HDCA along the downstream metabolism of CDCA, and CA, DCA, DCA-1β-ol, and DCA-5β-ol along the downstream metabolism of CA. The serum levels of BAs showed well consistency with the serum TBA data (Fig. 4A). The KTZ treatments did not significantly alter the serum levels of all BAs compared with the baseline data. However, almost all the studied BAs were significantly elevated at the induction phase compared with the baseline data. As shown in Fig. 4D, the KTZ treatments also did not significantly change the urinary BA levels at the inhibition phase, whereas the RFP treatments significantly increased their levels in urine at the induction phase, which showed well consistency with the serum data.

The levels of cortisol and 6β-OHF determined in urine and serum at the baseline phase, inhibition phase, and induction phase were shown in Fig. 4, E and F, respectively. Cortisol was detected in all urine and serum samples, whereas 6β-OHF was not detectable (lower than lower limit of quantitation, 5 ng/ml) in all serum samples and almost all the urine sample of the baseline and inhibition phases. Compared with the baseline data, the urinary levels of cortisol were not significantly changed by both KTZ and RFP treatments with a slightly increasing tendency. However, the serum levels of cortisol were significantly decreased by KTZ treatments and significantly increased by RFP treatments. Compared with the almost undetectable levels at the baseline phase and inhibition phase, the urinary levels of 6β-OHF were significantly elevated by RFP treatments.

Alteration of Metabolic Ratios of BA and Cortisol by KTZ and RFP. The secondary-to-primary ratios (LCA/CDCA and DCA/CA) and tertiary-to-secondary ratios (HDCA/LCA, DCA-1β-ol/DCA, and DCA-5β-ol/DCA) of BA metabolites in serum and urine were calculated and shown in Fig. 5, A and B. Along the downstream metabolism of CDCA, the serum ratios of LCA/CDCA and HDCA/LCA were not significantly changed by KTZ and RFP treatments in comparison with the baseline

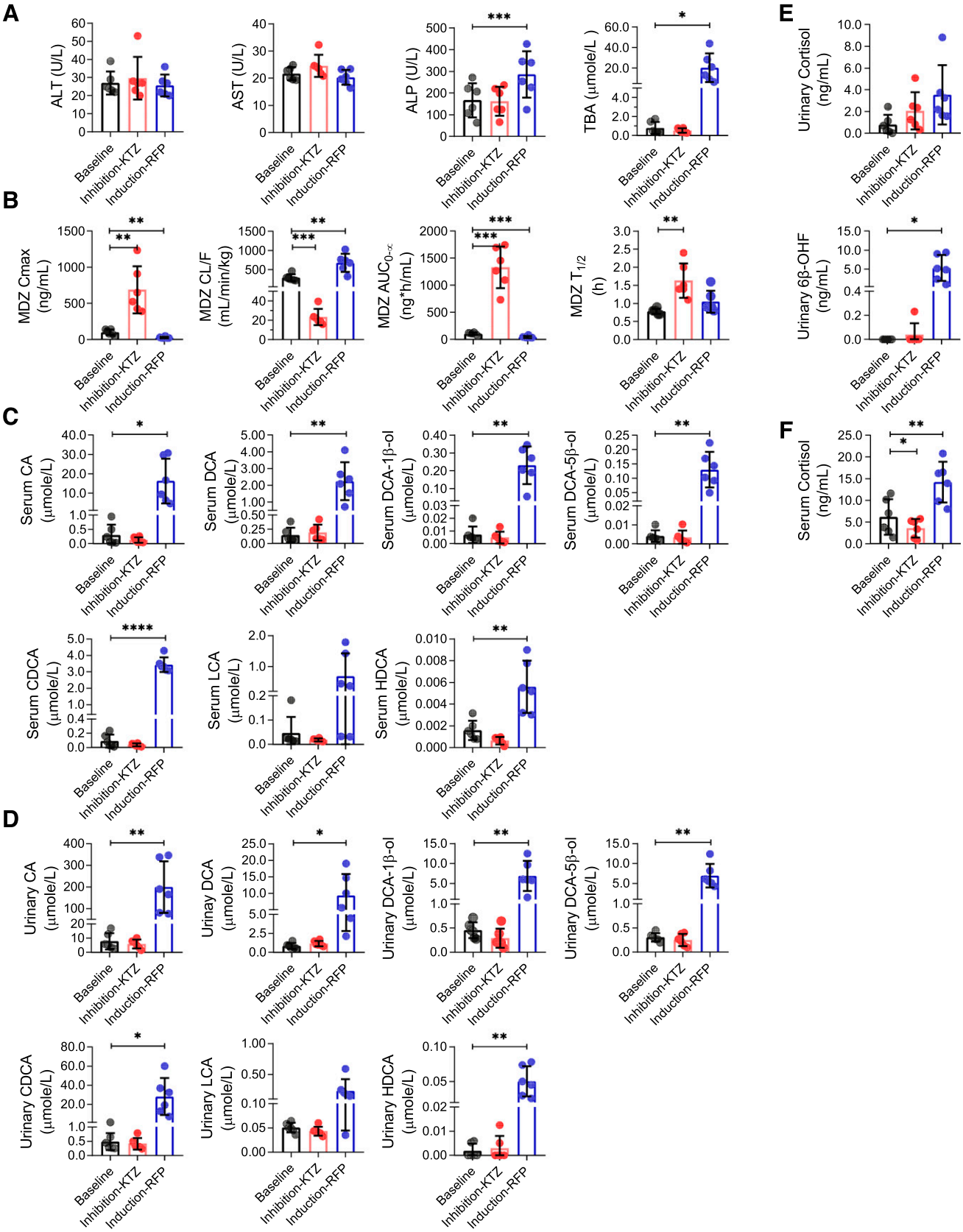

Fig. 4. Serum chemistry data (A), pharmacokinetic parameters of MDZ (B), predosing serum BA levels (C), urinary BA levels (D), urinary cortisol and 6β-OHF levels (E) and predosing serum cortisol levels (F) acquired at the last day of baseline, inhibition and induction phases. Data were shown as mean ± S.D. (n = 6). Paired-sample t tests were performed in comparison with the baseline data (*$P < 0.05$; **$P < 0.01$; ***$P < 0.001$).

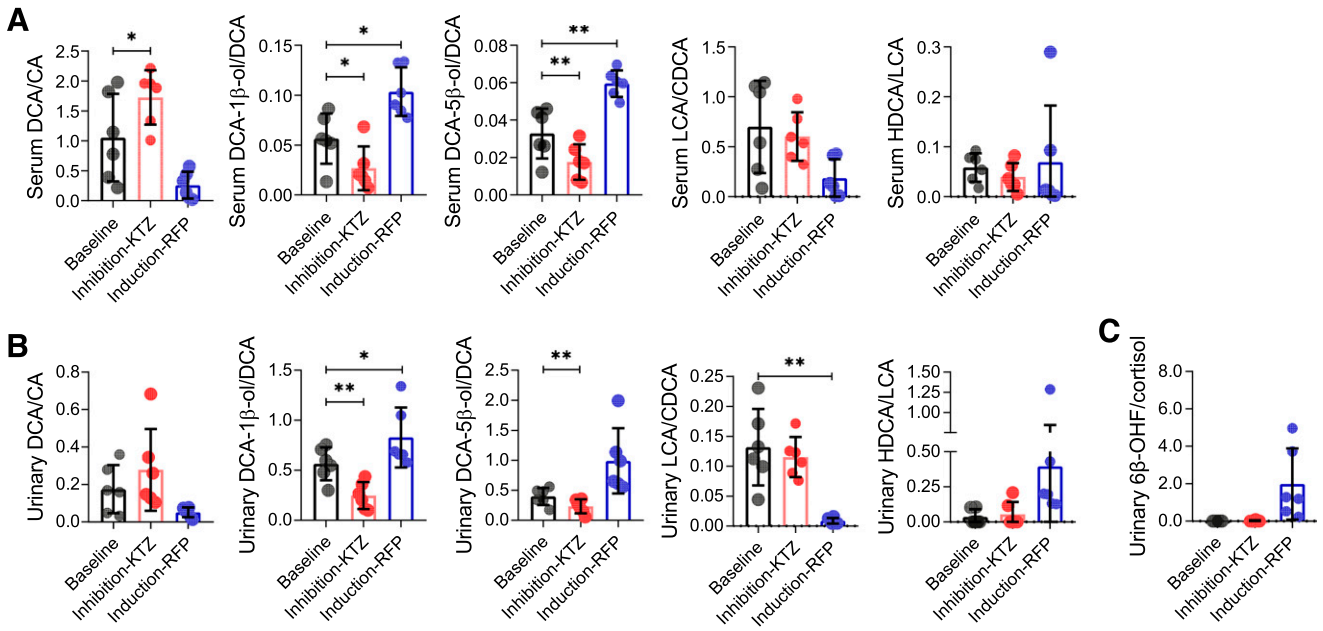

Fig. 5. Predosing serum BA metabolism ratios (A), urinary BA metabolism ratios (B), and urinary 6β-OHF/cortisol ratio (C) acquired at the last day of the baseline, inhibition, and induction phases. Data were shown as mean ± S.D. (n = 6). Paired-sample t tests were performed in comparison with the baseline data (*$P < 0.05$; **$P < 0.01$; ***$P < 0.001$).

data. Similar results were observed for the urinary LCA/CDCA and HDCA/LCA with the exception that the urinary LCA/CDCA was significantly decreased by RFP treatments. Along the downstream metabolism of CA, the tertiary-to-secondary ratios of BA metabolites were changed as expectations. Compared with the baseline data, the serum ratios of both DCA-1β-ol/DCA and DCA-5β-ol/DCA were significantly decreased and increased by KTZ and RFP treatments, respectively. Similar results were observed in the urinary DCA-1β-ol/DCA and DCA-5β-ol/DCA with less significance than the serum data. Corresponding to the inhibition and induction of DCA oxidative dispositions, the ratio of DCA/CA in serum and urine were increased and decreased with less statistical power by KTZ and RFP treatments, respectively. As for the metabolic ratio of 6β-OHF/cortisol, the urinary ratio at the inhibition phase remained unchanged in comparison with the baseline data because 6β-OHF was almost undetectable in these urine samples. The urinary ratio of 6β-OHF/cortisol was to some extent elevated by RFP treatments with only critical statistical significance (P = 0.0512).

Correlation of DCA Oxidation Ratios with Oral MDZ Clearance. Pearson correlation analysis was performed for the potential endogenous CYP3A biomarkers with the oral MDZ clearance data in dogs. As shown in Fig. 6A, a poor but significant interindividual positive correlation (r = 0.5072 and P = 0.0317) was observed between urinary 6β-OHF/cortisol and oral MDZ clearance, which was clearly attributed to the almost undetectable 6β-OHF in urine samples of the baseline and inhibition phases. As shown in Fig. 6, B and C, a stronger and more significant interindividual positive correlation was observed exactly as expected between MDZ clearance and either DCA-1β-ol/DCA (r = 0.6470 and P = 0.0037 for serum data; r = 0.5509 and P = 0.0178 for urinary data) or DCA-5β-ol/DCA (r = 0.8225 and $P < 0.0001$ for serum data; r = 07835 and P = 0.0001 for urinary data). The same data trend was observed while looking into the intraindividual correlation data of each dog. In consistency with the positive correlation between the tertiary-to-secondary ratios (DCA-1β-ol/DCA and DCA-5β-ol/DCA) and MDZ clearance, a significant interindividual negative correlation was observed between the DCA/CA ratio (r = −0.7424 and P = 0.0004 for serum data; r = −0.5370 and P = 0.0216 for urinary data) and oral MDZ clearance data (Fig. 6, B and C).

Discussion

This work has provided proof-of-concept preclinical evidence for the strategy of using tertiary BA metabolism as CYP3A biomarkers. This strategy was first proposed in 2016 by Hayes et al., 2016, who identified the CYP3A-catalyzed 1β-hydroxylation of DCA and found that the urinary ratio of DCA-1β-ol/DCA was considerably elevated in a patient treated with carbamazepine, a potent CYP3A inducer. Three years later, we completed mapping the CYP3A4/3A7 specifically catalyzed oxidation pathway of secondary BAs, DCA, GDCA, and TDCA, which occur regioselectively at C-3β, C-1β, C-6α, C-5β, C-4β, C-6β, and C-19 (Chen et al., 2019; Zhang et al., 2019). The disclosed pathways extend the biologic function of CYP3A into an inherent role in the host response to the stress of secondary BAs. As the major circulating secondary BA, DCA is continuously synthesized from CA in lower gut by gut flora, recovered into enterocytes and hepatocytes where CYP3A enzymes specifically express, reconjugated with glycine or taurine, and simultaneously oxidized selectively by CYP3A into hydroxylated metabolites, which are subsequently inclined to be excreted into urine (Zhang et al., 2019). Since DCA has the similar exogenous nature and disposition mechanisms as drugs, the oxidation ratios of DCA show theoretical advantage over genuine endogenous biomarkers, such as cortisol 6β-hydroxylation, to monitor the enterohepatic CYP3A activities.

Based on our recent studies on the species differences of BA redox metabolism (Lin et al., 2020), beagle dogs were chosen instead of murine animals to test the hypothesis because dogs have a similar BA metabolism network to humans. The decision forced us to confront an understudied area of drug metabolism in dogs, a species that is extensively used in human and veterinary drug development. Oral MDZ clearance was used as the reference of the in vivo CYP3A activities despite a dispute in literatures. Dogs were given a larger MDZ dose (1.5–2 mg/kg) than literatures (usually less than 1 mg/kg) because MDZ tablets (15 mg) for human use were used in this work. A short-term

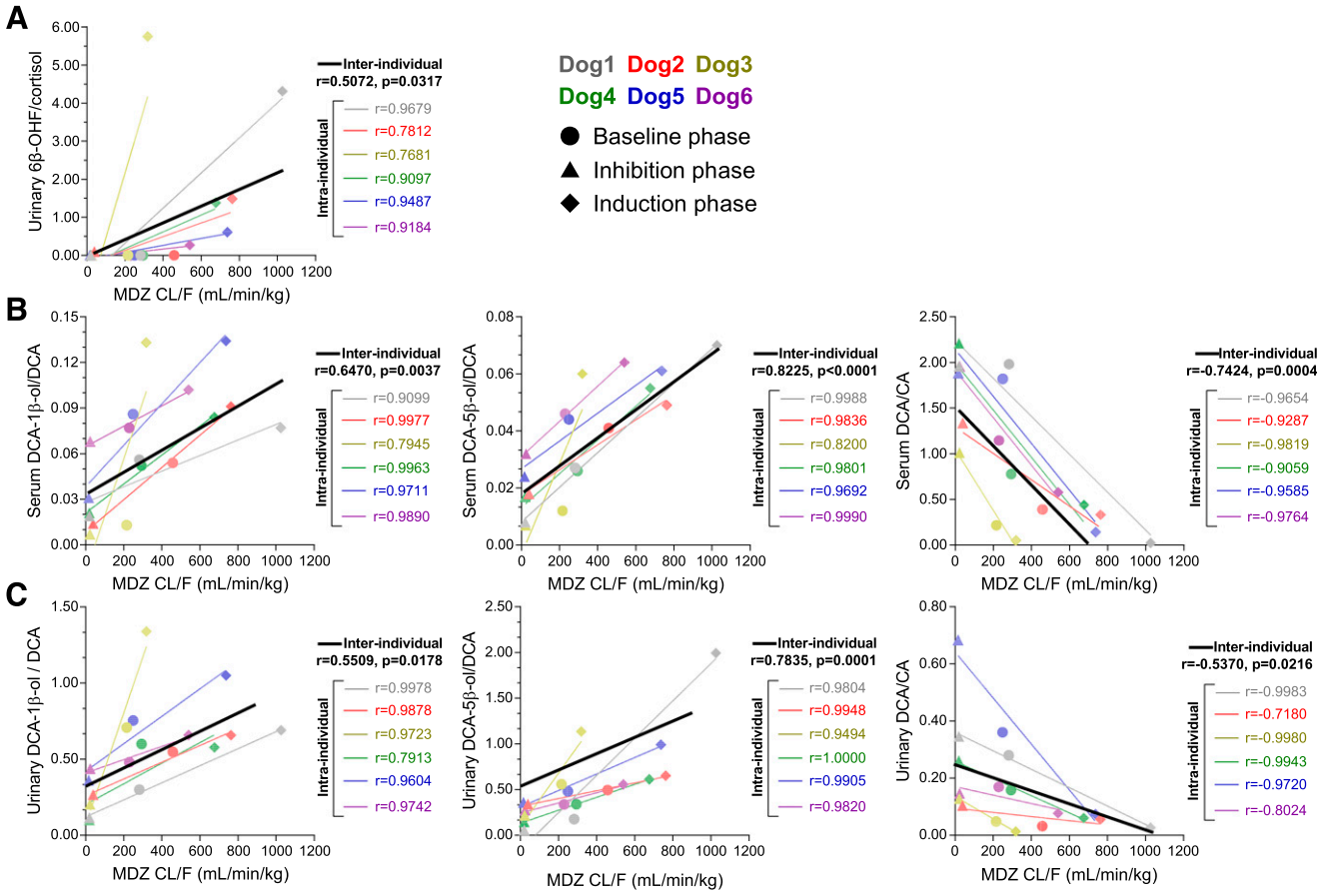

Fig. 6. Interindividual and intraindividual Pearson correlation analysis between the urinary 6β-OHF/cortisol ratio and oral MDZ clearance (A), the predosing serum BA ratios and oral MDZ clearance (B), and the urinary BA ratios and oral MDZ clearance (C).

intervention of oral KTZ (15 mg/kg, b.i.d. for 5 days) was employed to inhibit CYP3A with reference to the literature protocol (200 mg b.i.d. for 30 days) (Kuroha et al., 2002). The serum cortisol was significantly decreased by KTZ treatments, which was indicative of KTZ-induced transient hypoadrenocorticism (Hernandez-Bures et al., 2019; Sullivant and Lathan, 2020). A short-term intervention of oral RFP (300 mg, b.i.d. for 5 days) was used following the reference protocol (300 mg, b.i.d. for 22 days) (Abramson and Lutz, 1986). The RFP dose was higher than some studies (10 mg/kg, q.d.) (Nishibe et al., 1998; Kyokawa et al., 2001) to shorten the induction period and preliminarily investigate whether the marker efficacy was affected by the RFP-induced cholestasis, as shown by the significant increase of serum ALP and TBA compared with baseline data (Fig. 4A).

Since it is doubted whether MDZ is a sensitive probe for canine CYP3A due to mixed contribution of canine CYP2B11 and 3A12 to MDZ oxidations (Locuson et al., 2009; Mills et al., 2010), we repeated the reaction phenotyping of MDZ metabolism in recombinant canine P450 enzymes. The substrate concentrations at 4 and 40 μM were designed to cover the potential liver exposure of MDZ in the dog intervention studies. The same experiment was performed for DCA oxidation metabolism, which is known to be exclusively catalyzed by CYP3A4 and 3A7 in humans (Zhang et al., 2019). Among the eight tested canine P450s, the regioselective oxidation metabolism of DCA into DCA-1β-ol and DCA-5β-ol was exclusively catalyzed by CYP3A12 and 3A26, which was almost the same as the disclosed mechanism in humans. Inconsistent with the report of Locuson et al. (2009), however, the oxidative elimination of MDZ in dLMs was ascribed primarily to CYP3A12, secondly to CYP2B11 and CYP3A26, and minorly to CYP2C21. According to recent quantitative proteomic data, CYP3A12 rather than CYP2B11 is the most abundant P450 enzyme in both dog liver and intestines (Heikkinen et al., 2015). In contrast, CYP2C21 and 3A26 are expressed only in liver with much lower abundances than CYP3A12 and 2B11. Summarizing the reaction phenotyping data and the abundance data of CYPs in dog liver and intestines, we concluded that MDZ may serve as a valid in vivo probe of canine CYP3A at the tested dose.

In human studies, Shin et al. (2013, 2016) characterized that KTZ treatments (400 mg, q.d. for 4 days) caused about 5-fold reduction in the urinary 6β-OHF/cortisol ratio from the baseline data. For the first time as far as we know, we tried to investigate the marker efficacy of 6β-OHF/cortisol ratio for CYP3A activities. The attempt failed due to the extremely low activity of dog enzymes toward 6β-hydroxylation of cortisol. The serum levels of cortisol detected in our work were well consistent with the literature data (Ginel et al., 2012; Sieber-Ruckstuhl et al., 2015) but much lower than the human data (Kushnir et al., 2004; Lutz et al., 2010). Moreover, the serum and urinary levels of 6β-OHF in dogs were much lower than those of humans, which was well explained by cortisol 6β-hydroxylation not being detected in either dLM or canine P450 enzymes. Our data were also consistent with an early report, in which 6β-OHF or 6β-hydroxycortisone were not detected in dogs after intravenous administration of [1,2–^{3}H]cortisol (Miyabo et al., 1973). It was therefore proposed that the cortisol 6β-hydroxylation is not an appropriate CYP3A marker of dogs both in vitro and in vivo.

The enzyme-digestion technique was employed in this work to determine the total amount of each BA regardless of its conjugation patterns including *N*-acylamidation, glucuronidation, and sulfation

(Zhu et al., 2018). This method is rational because not only DCA but also GDCA and TDCA are selectively oxidized by CYP3A, and the oxidized metabolites are subsequently glucuronidated and/or sulfated (Zhang et al., 2019). Since DCA is mainly conjugated with glycine in humans and taurine in dogs (Thakare et al., 2018a,b), the tertiary oxidation ratios of GDCA and/or TDCA are also anticipated to be predictive of CYP3A activities. As shown in Fig. 4, the studies of urinary biomarkers may reduce the bioanalytical challenges because DCA-1β-ol and DCA-5β-ol are preferentially excreted in urine compared with DCA (Zhang et al., 2019). However, the urinary biomarker strategy inevitably involves variations derived from glucuronidation and/or sulfation metabolism of BAs and renal transport of the glucuronidated and/or sulfated BA metabolites, which was clearly indicated by the poorer interindividual correlation of urinary data than serum data in Fig. 6.

Despite the positive correlation between serum DCA oxidation biomarkers and MDZ clearance presented in this work (Fig. 6), the dynamic range of DCA oxidation biomarkers appear narrower than MDZ clearance. RFP treatments led to average 2- to 3-fold increases in both MDZ clearance and serum DCA oxidation markers, whereas KTZ treatments caused about 13- and 2-fold decreases in MDZ clearance and serum DCA oxidation markers, respectively. This could be explained by the DCA oxidation rate being much slower than the MDZ oxidation rate, resulting in high first-pass extraction of orally administered MDZ, which is sensitive to orally administered KTZ, a mixed inhibitor of canine CYP2B11, 2C21, and 3A12 (Mills et al., 2010). More preclinical studies involving interventions of weak to moderate to strong and more specific CYP3A inhibitors and inducers are required to disclose the dynamic range of DCA oxidation biomarkers to lay a solid foundation for the clinical validation studies.

In conclusion, since DCA is synthesized by gut microbiota, selectively oxidized via CYP3A, and subsequently disposed with similar mechanisms as exogenous drug molecules, the oxidative disposition of DCA may serve as novel biomarkers to instantly monitor the biologic fates of drug molecules disposed in similar pathways. After the concept, this work has provided the first proof-of-concept evidence that the predosing serum ratios of either DCA-1β-ol/DCA or DCA-5β-ol/DCA are predictive of the enterohepatic CYP3A activities in beagle dogs represented by oral MDZ clearance. Summarizing our recent studies focusing on the functional roles of CYP3A in tertiary metabolism of secondary BAs, we propose that the deeper understanding of biologic function of drug metabolism in host-gut microbial cometabolism homeostasis will become a promising scientific endeavor for future clinical pharmacology and therapeutics in the era of metagenomics.

Acknowledgments

We are grateful to Dr. Liang Xu (West China School of Pharmacy, Sichuan University) for his support of tertiary bile acids synthesis. We thank Jing Yang (Pharmacy Department of the Fourth People's Hospital of Chengdu) for gifting MDZ tablets and RFP capsules.

Authorship Contributions

Participated in research design: Lan.

Conducted experiments: Zeng, Gui, Tan, Zhu, Hu, Wu, Yang, Li, Lan.

Performed data analysis: Zeng, Gui, Tan, Zhu, Lan

Wrote or contributed to the writing of the manuscript: Zeng, Gui, Tan, Jia, Liu, Lan.

References

Abramson FP and Lutz MP (1986) The kinetics of induction by rifampin of alpha 1-acid glycoprotein and antipyrine clearance in the dog. *Drug Metab Dispos* **14**:46–51.

Bodin K, Bretillon L, Aden Y, Bertilsson L, Broomé U, Einarsson C, and Diczfalusy U (2001) Antiepileptic drugs increase plasma levels of 4beta-hydroxycholesterol in humans: evidence for involvement of cytochrome p450 3A4. *J Biol Chem* **276**:38685–38689.

Chen YJ, Zhang J, Zhu PP, Tan XW, Lin QH, Wang WX, Yin SS, Gao LZ, Su MM, Liu CX, et al. (2019) Stereoselective oxidation kinetics of deoxycholate in recombinant and microsomal CYP3A enzymes: deoxycholate 19-hydroxylation is an in vitro marker of CYP3A7 activity. *Drug Metab Dispos* **47**:574–581.

Diczfalusy U, Nylén H, Elander P, and Bertilsson L (2011) 4β-Hydroxycholesterol, an endogenous marker of CYP3A4/5 activity in humans. *Br J Clin Pharmacol* **71**:183–189.

Foti RS, Honaker M, Nath A, Pearson JT, Buttrick B, Isoherranen N, and Atkins WM (2011) Catalytic versus inhibitory promiscuity in cytochrome P450s: implications for evolution of new function. *Biochemistry* **50**:2387–2393.

Fraser DJ, Feyereisen R, Harlow GR, and Halpert JR (1997) Isolation, heterologous expression and functional characterization of a novel cytochrome P450 3A enzyme from a canine liver cDNA library. *J Pharmacol Exp Ther* **283**:1425–1432.

Galteau MM and Shamsa F (2003) Urinary 6beta-hydroxycortisol: a validated test for evaluating drug induction or drug inhibition mediated through CYP3A in humans and in animals. *Eur J Clin Pharmacol* **59**:713–733.

Ged C, Rouillon JM, Pichard L, Combalbert J, Bressot N, Bories P, Michel H, Beaune P, and Maurel P (1989) The increase in urinary excretion of 6 beta-hydroxycortisol as a marker of human hepatic cytochrome P450IIIA induction. *Br J Clin Pharmacol* **28**:373–387.

Ginel PJ, Sileo MT, Blanco B, Garfia B, and Quintavalla F (2012) Evaluation of serum concentrations of cortisol and sex hormones of adrenal gland origin after stimulation with two synthetic ACTH preparations in clinically normal dogs. *Am J Vet Res* **73**:237–241.

Gonzalez FJ (1990) Molecular genetics of the P-450 superfamily. *Pharmacol Ther* **45**:1–38.

Gorski JC, Hall SD, Jones DR, VandenBranden M, and Wrighton SA (1994) Regioselective biotransformation of midazolam by members of the human cytochrome P450 3A (CYP3A) subfamily. *Biochem Pharmacol* **47**:1643–1653.

Graham RA, Downey A, Mudra D, Krueger L, Carroll K, Chengelis C, Madan A, and Parkinson A (2002) In vivo and in vitro induction of cytochrome P450 enzymes in beagle dogs. *Drug Metab Dispos* **30**:1206–1213.

Gravel S, Chiasson JL, Gaudette F, Turgeon J, and Michaud V (2019) Use of 4β-hydroxycholesterol plasma concentrations as an endogenous biomarker of CYP3A activity: clinical validation in individuals with Type 2 diabetes. *Clin Pharmacol Ther* **106**:831–840.

Hayes MA, Li XQ, Grönberg G, Diczfalusy U, and Andersson TB (2016) CYP3A specifically catalyzes 1β-hydroxylation of deoxycholic acid: characterization and enzymatic synthesis of a potential novel urinary biomarker for CYP3A activity. *Drug Metab Dispos* **44**:1480–1489.

Heikkinen AT, Friedlein A, Matondo M, Hatley OJ, Petsalo A, Juvonen R, Galetin A, Rostami-Hodjegan A, Aebersold R, Lamerz J, et al. (2015) Quantitative ADME proteomics - CYP and UGT enzymes in the Beagle dog liver and intestine. *Pharm Res* **32**:74–90.

Hernandez-Bures A, White AG, and Riordan L (2019) Presumptive iatrogenic hypoadrenocorticism induced by high-dose ketoconazole administration in a dog. *J Vet Intern Med* **33**:2235–2238.

Kasichayanula S, Boulton DW, Luo WL, Rodrigues AD, Yang Z, Goodenough A, Lee M, Jemal M, and LaCreta F (2014) Validation of 4β-hydroxycholesterol and evaluation of other endogenous biomarkers for the assessment of CYP3A activity in healthy subjects. *Br J Clin Pharmacol* **78**:1122–1134.

Kim B, Lee J, Shin KH, Lee S, Yu KS, Jang IJ, and Cho JY (2018) Identification of ω- or (ω-1)-Hydroxylated medium-chain acylcarnitines as novel urinary biomarkers for CYP3A activity. *Clin Pharmacol Ther* **103**:879–887.

Kinirons MT, O'Shea D, Kim RB, Groopman JD, Thummel KE, Wood AJ, and Wilkinson GR (1999) Failure of erythromycin breath test to correlate with midazolam clearance as a probe of cytochrome P4503A. *Clin Pharmacol Ther* **66**:224–231.

Kuroha M, Azumano A, Kuze Y, Shimoda M, and Kokue E (2002) Effect of multiple dosing of ketoconazole on pharmacokinetics of midazolam, a cytochrome P-450 3A substrate in beagle dogs. *Drug Metab Dispos* **30**:63–68.

Kushnir MM, Neilson R, Roberts WL, and Rockwood AL (2004) Cortisol and cortisone analysis in serum and plasma by atmospheric pressure photoionization tandem mass spectrometry. *Clin Biochem* **37**:357–362.

Kyokawa Y, Nishibe Y, Wakabayashi M, Harauchi T, Maruyama T, Baba T, and Ohno K (2001) Induction of intestinal cytochrome P450 (CYP3A) by rifampicin in beagle dogs. *Chem Biol Interact* **134**:291–305.

Lan K, Su M, Xie G, Ferslew BC, Brouwer KL, Rajani C, Liu C, and Jia W (2016) Key role for the 12-hydroxy group in the negative ion fragmentation of unconjugated C24 bile acids. *Anal Chem* **88**:7041–7048.

Lin Q, Tan X, Wang W, Zeng W, Gui L, Su M, Liu C, Jia W, Xu L, and Lan K (2020) Species differences of bile acid redox metabolism: tertiary oxidation of deoxycholate is conserved in preclinical animals. *Drug Metab Dispos* **48**:499–507.

Locuson CW, Ethell BT, Voice M, Lee D, and Feenstra KL (2009) Evaluation of Escherichia coli membrane preparations of canine CYP1A1, 2B11, 2C21, 2C41, 2D15, 3A12, and 3A26 with coexpressed canine cytochrome P450 reductase. *Drug Metab Dispos* **37**:457–461.

Lutz U, Bittner N, Ufer M, and Lutz WK (2010) Quantification of cortisol and 6 beta-hydroxycortisol in human urine by LC-MS/MS, and gender-specific evaluation of the metabolic ratio as biomarker of CYP3A activity. *J Chromatogr B Analyt Technol Biomed Life Sci* **878**:97–101.

Martinez MN, Antonovic L, Court M, Dacasto M, Fink-Gremmels J, Kukanich B, Locuson C, Mealey K, Myers MJ, and Trepanier L (2013) Challenges in exploring the cytochrome P450 system as a source of variation in canine drug pharmacokinetics. *Drug Metab Rev* **45**:218–230.

Mealey KL, Martinez SE, Villarino NF, and Court MH (2019) Personalized medicine: going to the dogs? *Hum Genet* **138**:467–481.

Mills BM, Zaya MJ, Walters RR, Feenstra KL, White JA, Gagne J, and Locuson CW (2010) Current cytochrome P450 phenotyping methods applied to metabolic drug-drug interaction prediction in dogs. *Drug Metab Dispos* **38**:396–404.

Miyabo S, Kishida S, and Hisada T (1973) Metabolism and conjugation of cortisol by various dog tissues in vitro. *J Steroid Biochem* **4**:567–576.

Nishibe Y, Wakabayashi M, Harauchi T, and Ohno K (1998) Characterization of cytochrome P450 (CYP3A12) induction by rifampicin in dog liver. *Xenobiotica* **28**:549–557.

Patki KC, Von Moltke LL, and Greenblatt DJ (2003) In vitro metabolism of midazolam, triazolam, nifedipine, and testosterone by human liver microsomes and recombinant cytochromes p450: role of cyp3a4 and cyp3a5. *Drug Metab Dispos* **31**:938–944.

Rendic S and Guengerich FP (2015) Survey of human oxidoreductases and cytochrome P450 enzymes involved in the metabolism of xenobiotic and natural chemicals. *Chem Res Toxicol* **28**:38–42.

Rivory LP, Slaviero KA, Hoskins JM, and Clarke SJ (2001) The erythromycin breath test for the prediction of drug clearance. *Clin Pharmacokinet* **40**:151–158.
Rivory LP and Watkins PB (2001) Erythromycin breath test. *Clin Pharmacol Ther* **70**:395–399.
Russell DW (2003) The enzymes, regulation, and genetics of bile acid synthesis. *Annu Rev Biochem* **72**:137–174.
Shin KH, Ahn LY, Choi MH, Moon JY, Lee J, Jang IJ, Yu KS, and Cho JY (2016) Urinary 6β-hydroxycortisol/cortisol ratio most highly correlates with midazolam clearance under hepatic CYP3A inhibition and induction in females: a pharmacometabolomics approach. *AAPS J* **18**: 1254–1261.
Shin KH, Choi MH, Lim KS, Yu KS, Jang IJ, and Cho JY (2013) Evaluation of endogenous metabolic markers of hepatic CYP3A activity using metabolic profiling and midazolam clearance. *Clin Pharmacol Ther* **94**:601–609.
Sieber-Ruckstuhl NS, Burkhardt WA, Hofer-Inteeworn N, Riond B, Rast IT, Hofmann-Lehmann R, Reusch CE, and Boretti FS (2015) Cortisol response in healthy and diseased dogs after stimulation with a depot formulation of synthetic ACTH. *J Vet Intern Med* **29**:1541–1546.
Sullivant AM and Lathan P (2020) Ketoconazole-induced transient hypoadrenocorticism in a dog. *Can Vet J* **61**:407–410.
Thakare R, Alamoudi JA, Gautam N, Rodrigues AD, and Alnouti Y (2018a) Species differences in bile acids I. Plasma and urine bile acid composition. *J Appl Toxicol* **38**:1323–1335.
Thakare R, Alamoudi JA, Gautam N, Rodrigues AD, and Alnouti Y (2018b) Species differences in bile acids II. Bile acid metabolism. *J Appl Toxicol* **38**:1336–1352.
Wienkers LC and Heath TG (2005) Predicting in vivo drug interactions from in vitro drug discovery data. *Nat Rev Drug Discov* **4**:825–833.
Yin S, Su M, Xie G, Li X, Wei R, Liu C, Lan K, and Jia W (2017) Factors affecting separation and detection of bile acids by liquid chromatography coupled with mass spectrometry in negative mode. *Anal Bioanal Chem* **409**:5533–5545.
Zanger UM and Schwab M (2013) Cytochrome P450 enzymes in drug metabolism: regulation of gene expression, enzyme activities, and impact of genetic variation. *Pharmacol Ther* **138**:103–141.
Zhang J, Gao LZ, Chen YJ, Zhu PP, Yin SS, Su MM, Ni Y, Miao J, Wu WL, Chen H, et al. (2019) Continuum of host-gut microbial Co-metabolism: host CYP3A4/3A7 are responsible for tertiary oxidations of deoxycholate species. *Drug Metab Dispos* **47**:283–294.
Zhu P, Zhang J, Chen Y, Yin S, Su M, Xie G, Brouwer KLR, Liu C, Lan K, and Jia W (2018) Analysis of human C24 bile acids metabolome in serum and urine based on enzyme digestion of conjugated bile acids and LC-MS determination of unconjugated bile acids. *Anal Bioanal Chem* **410**:5287–5300.

Address correspondence to: Dr. Ke Lan, West China School of Pharmacy, Sichuan University, No. 17 People's South Rd., Chengdu, 610041 China. E-mail: lanwoco@scu.edu.cn